Appl. Phys. A 77, 163–166 (2003)
DOI: 10.1007/s00339-003-2099-3

Applied Physics A
Materials Science & Processing

D. ZHANG
C. LI
S. HAN
X. LIU
T. TANG
W. JIN
C. ZHOU✉

Ultraviolet photodetection properties of indium oxide nanowires

Dept. of E.E.-Electrophysics, University of Southern California, Los Angeles, CA 90089, USA

Received: 8 January 2003/Accepted: 9 January 2003
Published online: 28 March 2003 • © Springer-Verlag 2003

ABSTRACT Photoconducting properties of In_2O_3 nanowires were studied. Devices based on individual In_2O_3 nanowires showed a substantial increase in conductance of up to four orders of magnitude upon exposure to UV light. Such devices also exhibited short response times and significant shifts in the threshold gate voltage. The sensitivity to UV of different wavelengths was studied and compared. We have further demonstrated the use of UV light as a "gas cleanser" for In_2O_3 nanowire chemical sensors, leading to a recovery time as short as 80 s.

PACS 78.67

1 Introduction

One-dimensional nanostructures, such as nanowires and nanotubes, are the most promising materials for solid-state sensors due to their ultrahigh surface-to-volume ratios [1, 2]. In addition to chemical and biological sensing properties, their photodetection, or so-called optical switching properties [3], have also attracted much attention because an optical gating can work as an alternative to electrical gating for nanowire devices used in memory storage and logic circuits, where the performance critically relies on binary switching. Moreover, it has been found that the photosensitive characteristics of nanowires can greatly enhance the performance of some nanowire gas sensors by improving their sensitivities, as well as shortening the recovery time [4]. Light-enhanced gas sensing properties have been reported for SnO_2 nanoribbon sensors [4] and SnO_2/In_2O_3 thin-film sensors [5]. In sharp contrast, the photodetection and light-enhanced gas sensing properties of In_2O_3 nanowires have been rarely reported, presumably due to a lack of high-quality In_2O_3 nanowires in the past. Based on our recent success regarding the diameter-controlled synthesis of single-crystalline In_2O_3 nanowires [6], we have studied the UV response of devices consisting of individual nanowires. These devices showed sensitivities as high as 10^4 to UV light illumination, accompanied by substantial shifts in the gate threshold voltage. Differential response to UV illumination at different wavelengths has also been observed. We have further demonstrated the use of UV light as a "gas cleanser" for In_2O_3 nanowire chemical sensors after exposure to diluted NO_2 gas, leading to a recovery time as short as 80 s.

2 Experimental

In_2O_3 nanowires were synthesized via the vapor–liquid–solid mechanism, and details of the process can be found in our previous publication [6]. After the synthesis, scanning electron microscopy (SEM) and transmission electron microscopy (TEM) examination revealed that these nanowires had well-controlled diameters of around 10 nm and lengths exceeding 3 μm. A high-resolution TEM (HRTEM) image is shown in Fig. 1a. The lattice spacing along the [110] growth direction (0.72 nm) is in good agreement with the lattice constant for In_2O_3 (1.01 nm). The as-synthesized nanowires were deposited from a suspension in isopropyl alcohol onto a degenerately doped silicon wafer covered with 500-nm SiO_2. Photolithography and Ti/Au deposition were performed to pattern the drain and source electrodes to contact both ends of the individual wires. The Si substrate was used as a back gate in our electronic measurements. Figure 1b shows the SEM image of a device fabricated in this way, where an In_2O_3 nanowire bridging the source and the drain electrodes can be clearly seen. A double-wavelength (365 nm and 254 nm) UV lamp with a power dens-

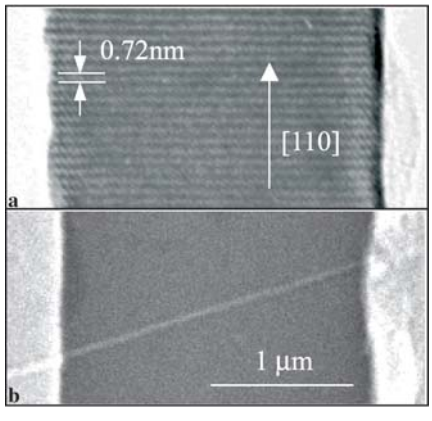

FIGURE 1 **a** HRTEM image of an In_2O_3 nanowire showing the [110] growth direction. The lattice spacing is consistent with the lattice constant for In_2O_3, which is 10.1 Å. **b** SEM image of the nanowire device used in our measurements

✉ Fax: +1-213/740-8677, E-mail: chongwuz@usc.edu

ity of approximately 3 mW/cm^2 was fixed approximately 1 cm away from the sample. The photoresponse of our devices was carried out under practical conditions – the devices were kept in air, at room temperature and under indoor incandescent light during the measurements.

3 Results and discussion

As shown in Fig. 2a, the current–voltage (I–V) curve of the nanowire device taken before the exposure to UV light indicates a relatively high resistance, where a differential conductance of only 3.6×10^{-1} nS is obtained for $V = 0$ V. The asymmetry in the I–V curve is a result of the local gating effect, as reported previously [7]. Upon exposure to UV of 365-nm wavelength, the device conductance increased immediately and stabilized after tens of seconds, leading to an I–V curve with a linear conductance around 1.7×10^3 nS, shown in Fig. 2a. The device became even more conductive after the device was exposed to UV of 254-nm wavelength, where a linear I–V curve with a conductance of 5.0×10^3 nS was observed, indicating a sensitivity of up to 10^4. We have also measured the current vs. gate voltage (I–V_g) characteristics of the device, with the source–drain bias fixed at 0.32 V, under various conditions, shown in Fig. 2b. In addition to the apparent change in the conductance, both the threshold gate voltage and the slope of the I–V_g curves were significantly modulated by the UV light. The threshold gate voltage shifted from +5 V for the initial unexposed state to −2 V and −25 V after exposure to 365-nm and 254-nm UV light, respectively. The change in the carrier concentrations can be estimated from the formula $\Delta n = C\Delta V_t/L$, where C and L represent the capacitance and length of the nanowire and ΔV_t is the shift in the threshold gate voltage. The capacitance can be estimated to be $C = 8.16 \times 10^{-5}$ pF for a 2-μm-long nanowire [6]. It is thus found that the carrier concentration was enhanced by 1.79 nm^{-1} and 7.65 nm^{-1} for the 365-nm and 254-nm UV light, corresponding to threshold-voltage shifts of −7 V and −30 V, respectively. The carrier mobility of the nanowire can be estimated from the I–V_g characteristics with the relation $dI/dV_g = \mu(C/L^2)V$. The different slopes of the three I–V_g curves in Fig. 2b give mobility values of 0.85 cm^2/V s, 6.1 cm^2/V s and 68 cm^2/V s, for the device without UV, with 365-nm UV and 254-nm UV, respectively. The above-mentioned analysis reveals an evident enhancement of both the carrier concentration and the mobility upon UV illumination, thus leading to the pronounced sensitivities we have observed.

To further explore the photoresponse properties, time-domain measurements were also carried out to evaluate the response speed of the nanowire. Figure 3a shows the current measured over time, where the 254-nm UV light was switched on and off repeatedly and a total of five cycles of data were recorded. We kept a constant drain–source voltage of 0.3 V and zero gate bias during the measurement. The conductance of the device was observed to increase rapidly upon UV exposure and decrease gradually once the UV was turned off. The device exhibited good reversibility between the high- and the low-conductivity states, as little drift was observed for both the "on" state and the "off" state after repeated exposure. The response time, which is defined as the time duration for a conductance change by one order of magnitude, was obtained to be approximately 10 s from this figure. Figure 3b shows the time-domain response of the device after it was exposed to 365-nm and 254-nm UV light sequentially. While 365-nm UV light brought the current to 33 nA, significantly more conduction (290 nA) was observed upon exposure to 254-nm UV light. This indicates that good selectivity between UV light of certain wavelengths can be readily achieved with our devices.

In_2O_3 nanowires are known to have a direct bandgap of 3.75 eV at $k = 0$ and an indirect energy gap of 2.62 V [8]. This explains the selectivity of our nanowire to those two different wavelengths we used. For the 254-nm UV light, each photon has an energy of 4.9 eV, sufficiently large to excite electrons directly from the valence band of the In_2O_3 nanowires to the conduction band at $k = 0$. In contrast, for the UV light with a peak wavelength at 365 nm, the majority of the photons have ener-

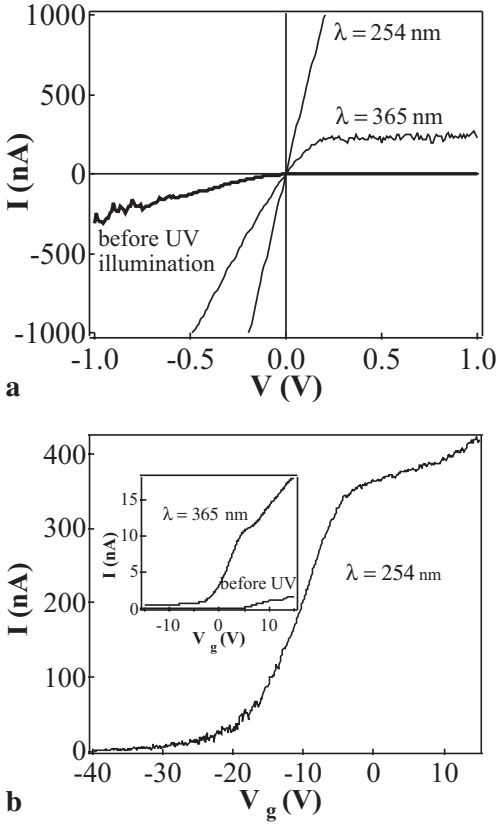

FIGURE 2 I–V curves (**a**) and I–V_g curves (**b**) recorded before UV light illumination and after exposure to UV light at wavelengths of 365 nm and 254 nm, respectively

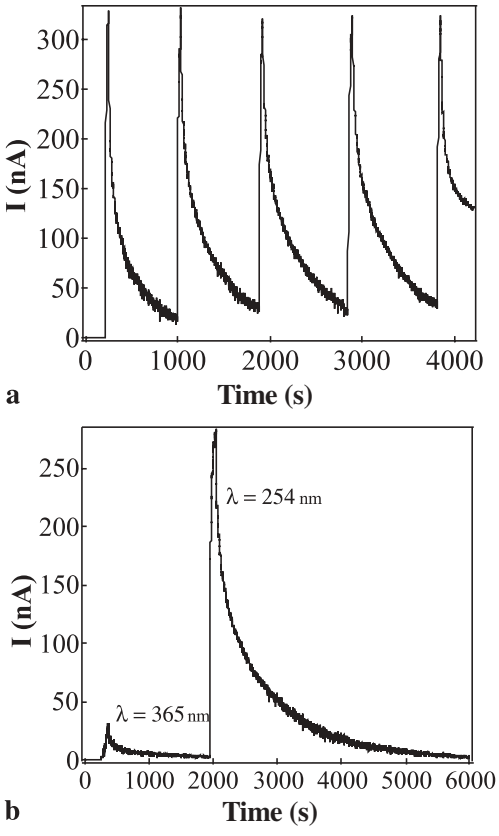

FIGURE 3 **a** Reversible switching of the nanowire between low- and high-conductivity states when the 254-nm UV light was turned on and off. **b** Photoresponse of the In_2O_3 nanowire to sequential UV illumination at wavelengths of 365 nm and 254 nm

gies below the In_2O_3 direct bandgap and hence the direct transition is prohibited. Though the indirect-forbidden transitions still exist with assisting phonons (~ 0.07 eV), their contribution to the conduction is limited due to the very small probability of simultaneous absorption of a photon and phonon [8]. However, there also exist some photons with higher energies due to the finite spectrum width, which can generate electron–hole pairs across the direct bandgap, thereby enhancing the conductance of the nanowire.

The physical principles underlying the photodetection properties of semiconducting metal oxides have been explained in many papers [3, 4, 9]. It is believed that two major mechanisms are active in the photoconductive In_2O_3 nanowires: First of all, because of the affinity between the electrons and the oxidizing O_2 molecules, O_2 can adsorb on the nanowire surface and combine with the nearby free electrons to form an O_2^- layer once the nanowire is exposed to air. This reduces the carrier concentration in the *n*-type In_2O_3 nanowire and thus suppresses its conductivity. Upon exposure to UV light, the O_2^- ions will recombine with the photogenerated holes and discharge O_2 molecules: $h^+ + O_2^- \rightarrow O_2$. This process helps erase the effect of the surrounding O_2 and brings the nanowire to the original electron-rich state. Secondly, further illumination will generate more electron–hole pairs in the conduction and valence bands, and these photogenerated carriers can significantly increase the conductance of the nanowire. In practice, since our measurements were taken in air, the influence of the ambient O_2 molecules existed all the time. The behavior of the nanowire is a result of the competing effects of both the O_2 molecules and the UV light.

Inspired by the interaction between the UV light, O_2 molecules and the nanowires, we have tried using UV light as a "cleanser" for our In_2O_3 nanowire gas sensors. Since the UV light can efficiently desorb ambient gas molecules from the nanowire surface, a short recovery time for the gas sensors was expected. Figure 4 shows a current-vs.-time curve we recorded with the nanowire device mounted in a sealed chamber. The device was biased at 0.05 V with the gate electrode fixed at 0 V. The chamber was pumped to high vacuum before the measurement. The current maintained a constant level (13.5 nA) until the device was exposed to the 254-nm UV light (point a), and then rose rapidly during the illumination. We turned off the lamp at $t = 200$ s (point b) and turned on an Ar gas flow simultaneously. This led to a small drop in the current due to the recombination of electrons and holes. 0.1% NO_2 gas was added to the pure Ar flow at point c. The current showed a sharp decrease upon exposure to NO_2, as NO_2 can adsorb on the nanowire surface and withdraw electrons from the nanowire to form NO_2^-. We stopped the NO_2 supply at time $t = 600$ s (point d), and then turned off Ar flow and pumped the system at time $t = 700$ s (point e). However, as shown in the figure, neither Ar flow nor pumping could desorb the NO_2 molecules adsorbed on the nanowire surface in an effective manner, and the device remained in the highly resistive state. To effectively recover the sensor, we turned on the UV lamp again (point f). The UV light illumination immediately brought the device back to the high-conducting state. We repeated this process (from b to f) again. The highly reversible behavior of the device is explicitly shown in

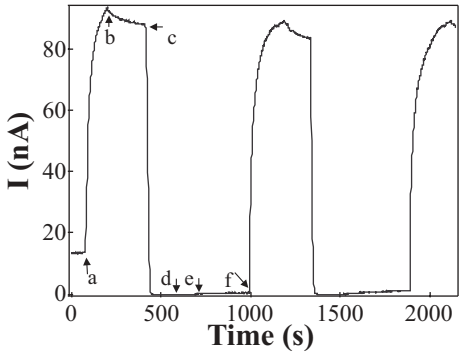

FIGURE 4 Two NO_2 gas sensing cycles

the figure. The application of UV light significantly shortened this "cleaning" process and reduced the recovery time of the sensor to only 80 s. This example perfectly reveals light-enhanced desorption kinetics in the nanowire systems.

4 Conclusion

In conclusion, we have investigated the photoresponse of In_2O_3 nanowires under UV illumination. Our In_2O_3 nanowire devices exhibited significantly enhanced conduction under UV exposure and sensitivities as high as 10^4 were achieved. UV illumination at two wavelengths (254 nm and 365 nm) gave sharply different results as the photon energy must be greater than the In_2O_3 bandgap to generate electron–hole pairs. Finally, UV illumination has been demonstrated to work as a gas cleanser for In_2O_3 nanowires working as NO_2 sensors, with a recovery time of approximately 80 s.

ACKNOWLEDGEMENTS The authors thank Dr. J. Han and Dr. M. Meyyapan of NASA Ames Research Center for valuable technical discussions. Prof. E. Goo, Prof. M. Gundersen and Dr. X. Zhang are acknowledged for their help with the material synthesis and characterization. This work was supported by USC, NASA Contract No. NAS2-99092, a NSF CAREER award, the NSF CENS program and a Zumberger award.

REFERENCES

1 J. Kong, N.R. Franklin, C. Zhou, M.G. Chapline, S. Peng, K. Cho, H. Dai: Science **287**, 622 (2000)
2 Y. Cui, Q. Wei, H. Park, C.M. Lieber: Science **293**, 1289 (2001)
3 H. Kind, H. Yan, B. Messer, M. Law, P. Yang: Adv. Mater. **14**, 158 (2002)
4 M. Law, H. Kind, B. Messer, F. Kim, P. Yang: Angew. Chem. Int. Ed. **41**, 2405 (2002)
5 E. Comini, A. Cristalli, G. Faglia, G. Sberveglieri: Sens. Actuators B **65**, 261 (2000)
6 C. Li, D. Zhang, S. Han, X. Liu, T. Tang, C. Zhou: Adv. Mater. **15**, 143 (2003)
7 D. Zhang, C. Li, S. Han, X. Liu, T. Tang, W. Jin, C. Zhou: Appl. Phys. Lett. **82**, 112 (2003)
8 R.L. Weiher, R.P. Ley: J. Appl. Phys. **37**, 299 (1966)
9 C. Xirouchaki, G. Kiriakidis, T.F. Pedersen, H. Fritzsche: J. Appl. Phys. **79**, 9349 (1996)